

Flexible 3D Cell-Based Platforms for the Discovery and Profiling of Novel Drugs Targeting *Plasmodium* Hepatic Infection

Francisca Arez,^{†,‡,§} Sofia P. Rebelo,^{†,‡,§} Diana Fontinha,^{§,■} Daniel Simão,^{†,‡} Tatiana R. Martins,^{†,‡} Marta Machado,[§] Christoph Fischli,^{||,⊥} Claude Oeuvray,[¶] Lassina Badolo,[□] Manuel J. T. Carrondo,^{†,‡} Matthias Rottmann,^{||,⊥} Thomas Spangenberg,^{¶,Ⓜ} Catarina Brito,^{†,‡} Beatrice Greco,^{*,¶} Miguel Prudêncio,^{*,§} and Paula M. Alves^{*,†,‡,Ⓜ}

[†]iBET, Instituto de Biologia Experimental e Tecnológica, Apartado 12, 2780-901 Oeiras, Portugal

[‡]Instituto de Tecnologia Química e Biológica António Xavier, Universidade Nova de Lisboa, Avenida da República, 2780-157 Oeiras, Portugal

[§]Instituto de Medicina Molecular João Lobo Antunes, Faculdade de Medicina, Universidade de Lisboa, 1649-028 Lisboa, Portugal

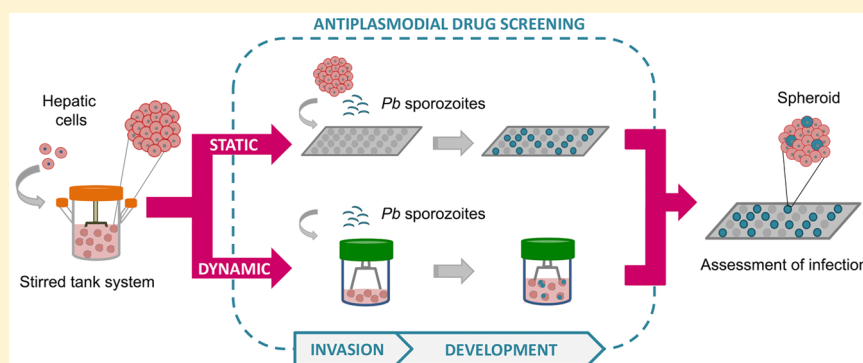
^{||}Swiss Tropical and Public Health Institute, Basel 4051, Switzerland

[⊥]University of Basel, Basel 4003, Switzerland

[¶]Global Health Institute of Merck, Ares Trading S.A., a subsidiary of Merck KGaA, Darmstadt, Germany, 1262 Eysins, Switzerland

[□]Discovery and Development Technologies, Merck Healthcare KGaA, Frankfurter Strasse 250, 64293 Darmstadt, Germany

Supporting Information



ABSTRACT: The restricted pipeline of drugs targeting the liver stage of *Plasmodium* infection reflects the scarcity of cell models that mimic the human hepatic phenotype and drug metabolism, as well as *Plasmodium* hepatic infection. Using stirred-tank culture systems, spheroids of human hepatic cell lines were generated, sustaining a stable hepatic phenotype over 4 weeks of culture. Spheroids were employed in the establishment of 3D *Plasmodium berghei* infection platforms that relied on static or dynamic culture conditions. *P. berghei* invasion and development were recapitulated in the hepatic spheroids, yielding blood-infective merozoites. The translational potential of the 3D platforms was demonstrated by comparing the *in vitro* minimum inhibitory concentration of M5717, a compound under clinical development, with *in vivo* plasma concentrations that clear liver stage *P. berghei* in mice. Our results show that the 3D platforms are flexible and scalable and can predict the efficacy of antiplasmodial therapies, constituting a powerful tool for integration in drug discovery programs.

KEYWORDS: 3D cell models, liver stage infection, malaria, *Plasmodium*, drug discovery, *in vitro*

Malaria is one of the deadliest human infectious diseases worldwide, having caused an estimated total of 435 000 deaths in 2017.¹ The disease is caused by protozoan parasites of the *Plasmodium* genus, of which five species, *Plasmodium falciparum* (Pf), *P. vivax* (Pv), *P. ovale* (Po), *P. malariae*, and *P. knowlesi*, are known to infect humans. The initial, obligatory phase of *Plasmodium* infection in the mammalian host occurs in the liver, where each sporozoite traverses several hepatocytes until productively invading one.² Inside the hepatocytes, sporozoites differentiate into exoerythrocytic

forms (EEFs) that replicate into thousands of mature blood-infective merozoites. Once released into the bloodstream, merozoites infect erythrocytes, leading to the malaria-associated pathology.³ The clinically silent nature of *Plasmodium*'s initial and obligatory developmental phase in the liver makes this stage of infection an attractive target for prophylactic intervention. Furthermore, it is in the liver that Pv

Received: April 18, 2019

Published: September 3, 2019

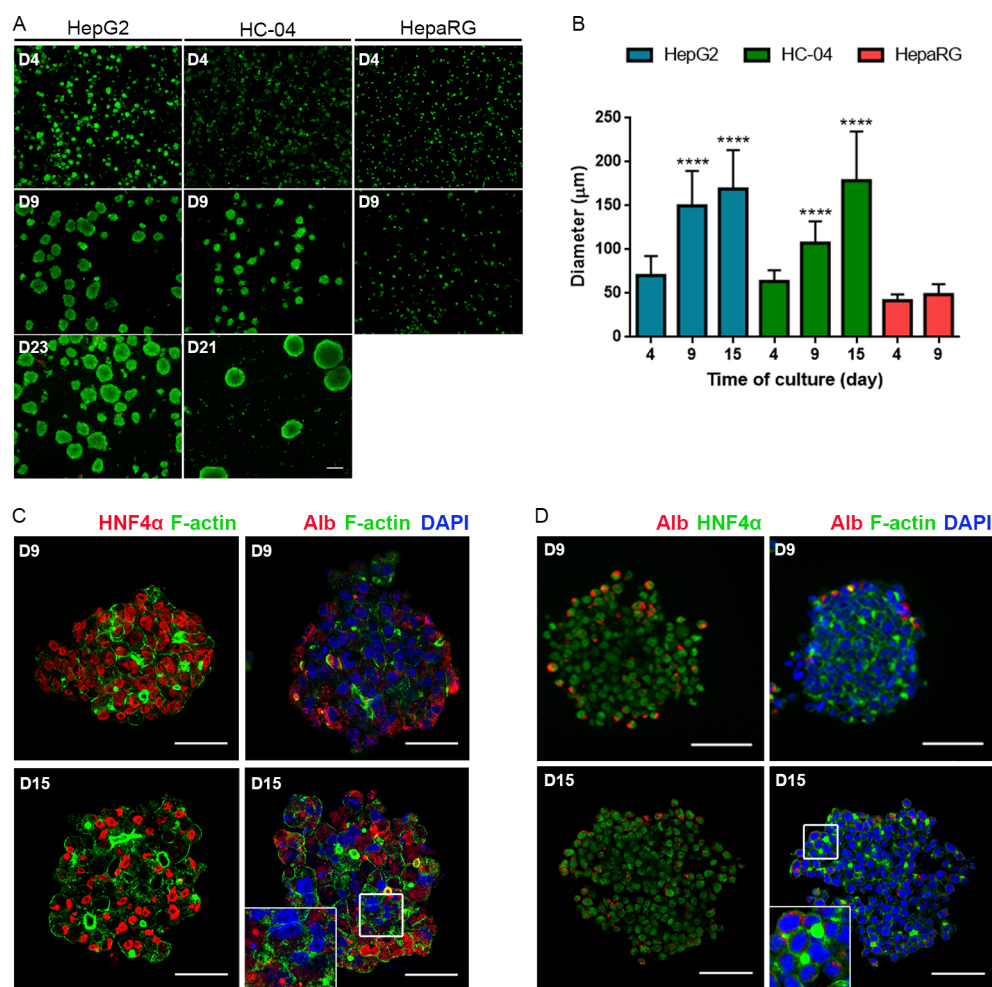


Figure 1. Characterization of HepG2, HC-04, and HepaRG cell lines in stirred culture systems. (A) Cell viability assay (fluorescein diacetate (FDA), green; TO-PRO-3, red) at days 4, 9, and 21 (HC-04) or 23 (HepG2) of culture. Scale bar: 200 μm . (B) Spheroid diameters at days 4, 9, and 15 of culture. Data are represented as mean \pm SD of at least 170 spheroids from two to five independent cultures for days 4, 9, and 15 of culture. Statistical analysis was performed by one-way ANOVA in comparison with day 4 of culture, followed by Tukey's multicomparison test (**** $p < 0.0001$). (C,D) Phenotypic characterization by fluorescence microscopy of day 9 and day 15 spheroids: (C) HepG2 and (D) HC-04. Hepatic phenotypic markers detected include albumin (Alb), F-actin, and HNF4 α . The insets in the bottom-right images highlight the membrane accumulation of F-actin, indicating cell polarization. Scale bars: 50 μm .

and *Po* parasites generate latent forms known as hypnozoites, which can remain dormant for months or years, until their activation leads to disease relapse.⁴

Because of the limitations inherent to addressing the liver stage of *Plasmodium* infection experimentally, including the scarcity of liver-stage models and the limited access to hypnozoite-forming parasites, few antiparasitic therapies target this phase of the parasite's life cycle. Among the therapies that target this phase are 8-aminoquinolines (e.g., primaquine and tafenoquine), the folate inhibitors sulfadoxine-pyrimethamine and atovaquone (ATO), and a naphthoquinone inhibitor of the malaria parasite's electron transport chain cytochrome bc1 complex (reviewed by Raphemot et al.⁵). The genetic diversity of *Plasmodium* parasites has led to the acquisition of resistance to the latter two of these drugs.^{5,6} Therefore, to fulfill the current therapeutic gaps in the malaria eradication agenda, new candidates that can be employed in single-dose treatments are required.^{7,8} DDD107498 (M5717), a drug candidate targeting *Plasmodium* eukaryotic translation elongation factor 2, may fulfill the potential single-dose requirement in terms of curing and preventing infection and

blocking transmission of malaria. This compound has a long plasma half-life and displays potent activity against both liver- and blood-stage parasites, as well as male and female gametocytes.⁹

Despite the efforts to develop new drug candidates that target the liver stage of *Plasmodium* infection, the restricted pipeline of antiparasitic drugs acting on this phase of infection reflects the scarcity of preclinical *in vitro* models suitable for studying: (i) the complex biology of *Plasmodium* development, (ii) drug efficacy, (iii) drug metabolism, and (iv) toxicology.¹⁰ Preclinical *in vitro* models for the discovery of antiparasitic drugs targeting the liver stage of infection rely mostly on primary human hepatocytes (PHH) cultured in formats that sustain *Pv* and *Pf* infection.^{11–14} These platforms depend on extracellular matrix cues (e.g., collagen type I) or murine fibroblasts to sustain hepatocyte polarization and functionality, which are not attained in conventional 2D culture systems.^{15,16} However, the phenotypic stability of these culture formats is still limited.^{17,18} Moreover, the use of PHH is restricted by their high cost and limited availability and the great variability between lots. Conversely, cell-line-derived

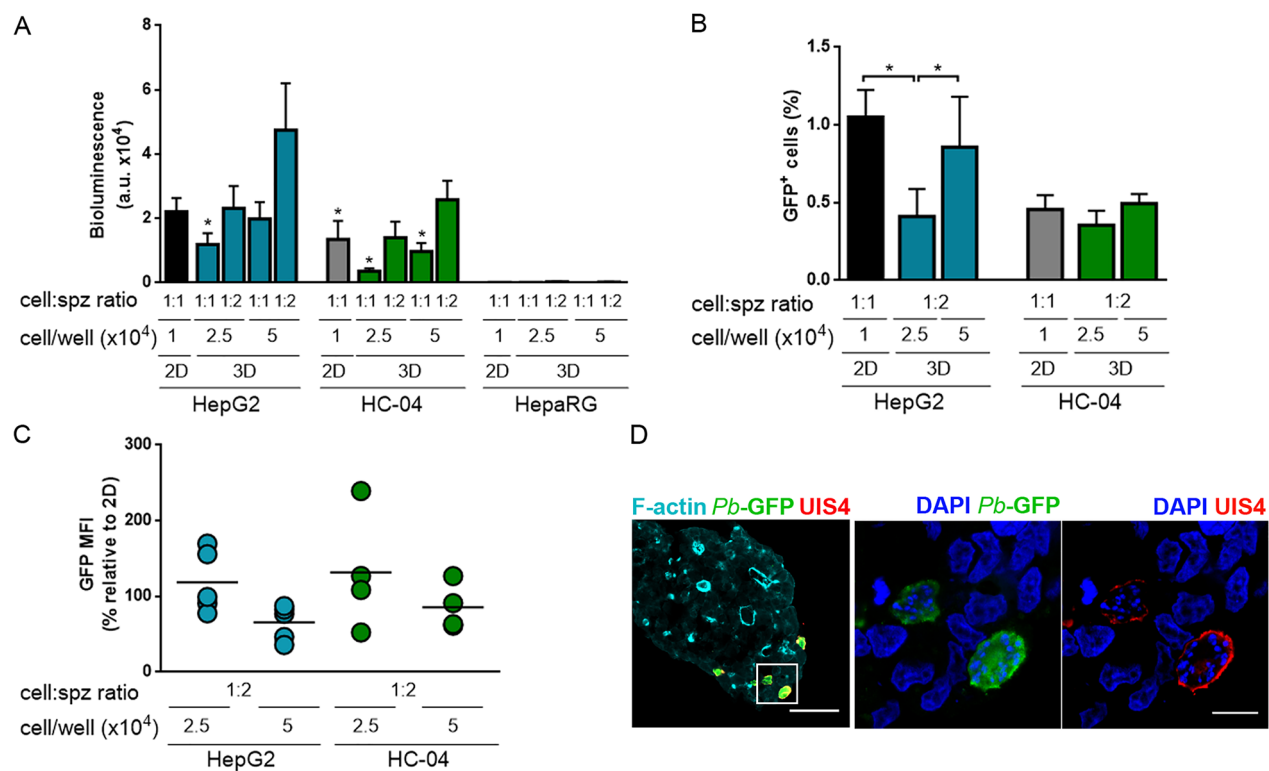


Figure 2. Infection of hepatic cell lines with *Plasmodium berghei* (*Pb*). (A) Bioluminescence values expressed in arbitrary units (a.u.) of *Pb*-Luc-infected HepG2, HC-04, and HepaRG cells, determined by measuring luciferase activity. Results are represented as mean \pm SEM of at least three independent experiments. Statistical analysis with paired *t* tests was performed for both HepG2 and HC-04 relative to 2D HepG2 ($*p < 0.05$). (B) Percentage of cells infected by *Pb*-GFP for HepG2 and HC-04. Results show the percentage of GFP-positive cells quantified by flow cytometry, represented as the mean \pm SEM of at least three independent experiments. Statistical analysis by paired *t* tests was performed by comparing all conditions ($*p < 0.05$). (C) *Pb* development in HepG2 and HC-04 cells, determined by measurement of the geometric mean of GFP fluorescence intensity (MFI). Data represent the mean \pm SEM of at least three independent cultures. Statistical analysis was performed by one-way ANOVA, followed by Tukey's multicomparison test. (D) Parasitophorous vacuole membrane detection shown by staining of the UIS4 membrane protein in *Pb* parasites developing inside HepG2 spheroids. Scale bar: 50 μ m. The inset represents a zoom-in of one stack of UIS4 staining. Scale bar: 10 μ m.

spheroids, in which cell–cell interactions are maximized, have been shown to promote the accumulation of native ECM and improve liver-specific features, such as the expression of polarity proteins and the membrane localization of phase III transporters;^{19–22} thus, they more closely resemble the *in vivo* architecture and functionality of the hepatic lobule. HepG2, a cell line with lower metabolic performance than HepaRG and PHH,²³ has been shown to present improved expression of metabolic enzymes when cultured as spheroids.²⁴ Both HepG2 and HepaRG spheroids have been used in drug testing platforms and display enhanced sensitivity for the determination of drug cytotoxicity, mainly with repeated drug dosing.^{19,20,22,24–26} The use of stirred-tank systems to generate spheroids provides a homogeneous physicochemical culture environment that maintains 3D hepatocyte cultures for longer periods of time,^{27,28} with the possibility of noninvasive sampling throughout culture time and upscaling,^{29,30} constituting a cost-effective alternative.

The present work focuses on the development of 3D cell-based *Plasmodium* hepatic infection platforms, relying on spheroids of human hepatic cell lines generated in stirred-tank culture systems, for the discovery of novel antiplasmodial drugs. *Plasmodium* infection of the hepatic spheroids was optimized in both static and dynamic cell suspension conditions. The 3D infection platforms were used to assess the efficacy of two antiplasmodial drugs with distinct modes of action, M5717 and ATO, throughout hepatic infection by

rodent *Plasmodium berghei* (*Pb*) parasites. The translational potential of these platforms was assessed by comparing these results with those obtained from *in vivo* studies. Our results show the applicability of these novel platforms for drug discovery programs, given their scalability, flexibility, and cost-effectiveness.

RESULTS

Production of 3D Hepatic Cell Models in Stirred-Tank Culture Systems. For the generation of hepatic spheroids, three hepatic cell lines, HepG2, HC-04, and HepaRG, were selected on the basis of their drug metabolic activities, susceptibility to *Plasmodium* infection, or both.^{11,23,31} All cell lines were inoculated as single cell suspensions in spinner vessels, and their aggregation was optimized to attain high cell packing densities, to promote the formation of compact spheroids. The inoculum cell density, stirring rate, and serum concentration were adjusted as previously described.^{27,30} The parameters optimized for each cell line are presented in [Supplementary Table S1](#). By day 4, cultures of the three cell lines were mainly composed of compact spheroids ([Figure 1A](#)). HepG2 and HC-04 spheroids presented high cell viability after 21 days of culture ([Figure 1A](#)) and could be maintained for at least 30 days. At day 4 after inoculation, HepG2, HC-04, and HepaRG spheroids displayed average diameters of 70 ± 22 , 63 ± 13 , and 42 ± 7 μ m, respectively ([Figure 1B](#)). Although HepaRG spheroids maintained similar average

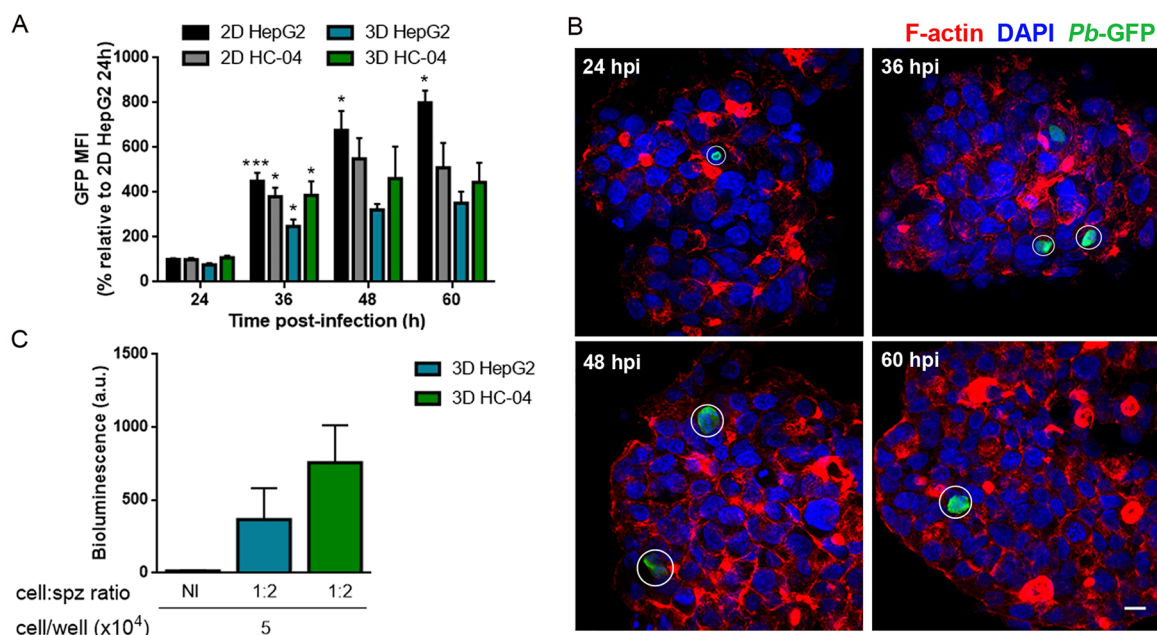


Figure 3. Characterization of *P. berghei* development in 3D cultures. (A) *Pb*-GFP development at 24, 36, 48, and 60 hours post infection (hpi) analyzed by flow cytometry of 5.0×10^4 cell/well HepG2 and HC-04 spheroids infected at a 1:2 cell/sporozyte (spz) ratio (. Results are represented as the mean \pm SEM of three independent replicates. A paired *t* test was performed for each condition relative to the previous time point (* $p < 0.05$, *** $p < 0.001$). (B) *Pb*-GFP development at 24, 36, 48, and 60 hpi assessed by confocal imaging. Scale bars: 10 μ m. (C) Merozoite release as indicated by bioluminescence detection in supernatants of spheroids at 5.0×10^4 cell/well infected by *Pb*-Luc at a 1:2 cell/spz ratio. Noninfected (NI) 3D cultures were used as negative control. Results are represented as bioluminescence arbitrary units (a.u.) measured by luciferase activity (mean \pm SEM from three independent experiments).

diameters throughout culture time, the diameters of the HepG2 and HC-04 spheroids increased up to 169 ± 45 and $179 \pm 56 \mu\text{m}$ by day 15 (Figure 1B). The hepatic phenotype in the spheroids was analyzed by the characterization of cell polarization and hepatocyte-specific markers. F-actin filaments were detected adjacent to the cell membrane in the apical regions of the cells from day 9 to day 15 of culture (Figure 1C,D) forming bile-canalculi-like structures typical of polarized hepatic cells.^{19,22,28} The membrane accumulation of E-cadherin corroborates the cell polarization observed at day 9 of culture (Figure S1). The hepatic identities and biosynthetic functions of HepG2 and HC-04 spheroids were further corroborated by the presence of the hepatocyte nuclear factor 4 α (HNF4 α) and of the liver biosynthetic globular protein albumin (Alb) by days 9 and 15 of culture (Figure 1C,D).

Infection of 3D Hepatic Spheroids with *Plasmodium berghei*. For the implementation and optimization of a 3D *Plasmodium* infection platform, the *Pb* infection procedure in 2D (described in Prudêncio, Mota, and Mendes³²) was adapted to infect spheroids in a 96-well plate format (static infection, Figure S2A). Therefore, 2D HepG2 cells plated at 1×10^4 cell/well and infected by *Pb* in a 1:1 cell/sporozyte (spz) ratio were used as an infection control in all experiments. Spheroids from days 4 and 9 were infected by *Pb*-Luc in different conditions (data not shown). Spheroids from day 9 were more homogeneous than those from day 4 and led to higher parasite loads and were therefore selected for optimization of infection parameters in 3D. Parameters influencing hepatic infection and spheroid morphology were evaluated by employing HepG2 spheroids. To this end, cell densities of 1×10^4 , 2.5×10^4 , and 5×10^4 cell/well with cell/spz ratios of 2:1, 1:1, and 1:2 were assessed using luciferase-expressing rodent *Pb* parasites (*Pb*-Luc, Figure S2B,C). Given

the surface area covered, the morphology of the spheroids observed under static conditions, and the parasite load estimated, cell concentrations of 2.5×10^4 and 5×10^4 cell/well and cell/spz ratios of 1:1 and 1:2 were selected for further studies. Therefore, spheroids of the three cell lines from day 9 of culture were infected with *Pb*-Luc by employing the four infection conditions selected (Figure 2). Forty-eight hours postinfection (hpi), the luciferase activity of HepG2 spheroids was similar to that of the 2D HepG2 cells for all the conditions tested, except for that at the concentration of 2.5×10^4 cell/well with 1:1 cell/spz, which was significantly lower than that of the latter ($41 \pm 13\%$ of 2D HepG2). HC-04 cells presented lower parasite loads than 2D HepG2 in 2D and 3D at a cell/spz ratio of 1:1 ($58 \pm 12\%$ for 2D, and 21 ± 3 and $57 \pm 9\%$ for spheroids at 2.5×10^4 and 5×10^4 cell/well). At a cell/spz ratio of 1:2, the parasite loads were 72 ± 26 and $126 \pm 17\%$ of that observed in 2D HepG2 cells for 2.5×10^4 and 5×10^4 cell/well, respectively. In summary, both HepG2 and HC-04 spheroids sustained infection by *Pb* sporozoites in the four selected conditions, with higher amounts of spz and higher cell densities leading to higher parasite loads, suggesting that the conditions optimized for HepG2 can be translated to the HC-04 cell system. On the other hand, the HepaRG cell line was not infected by *Pb*, either in the 2D or in the 3D formats (Figure 2A), suggesting that HepaRG does not sustain infection by rodent *Pb* parasites.

In order to further characterize *Pb* infection of 3D spheroids of HepG2 and HC-04 cells, a *Pb* strain constitutively expressing green fluorescent protein (*Pb*-GFP) was employed. This strain enables the quantification of GFP⁺ cells and GFP intensity by flow cytometry as surrogate measures of infection rate and parasite development, respectively.³³ *Pb*-GFP-infected 2D HepG2 cells, employed as controls, presented an average of

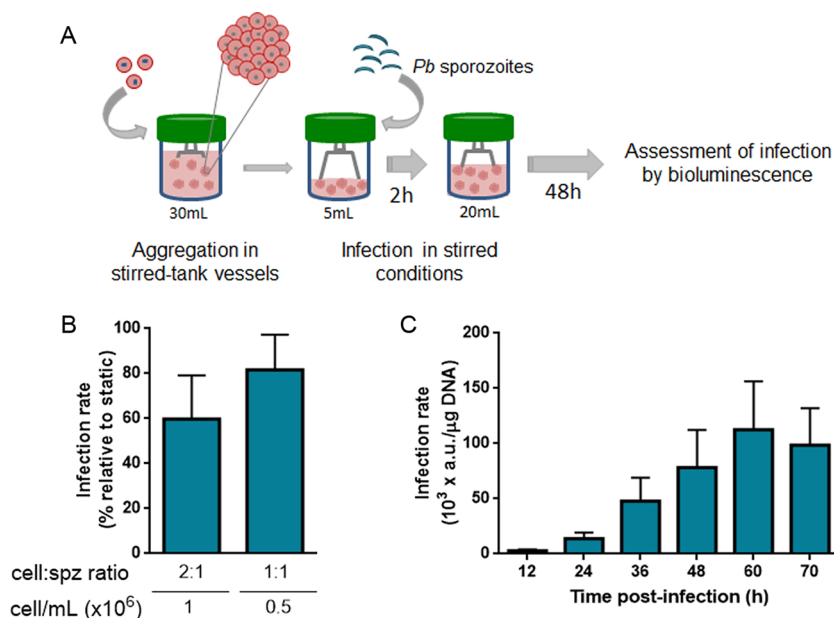


Figure 4. Characterization of *P. berghei* dynamic infection. (A) Schematic representation of the dynamic infection strategy (not at scale). (B) Infection rate of HepG2 spheroids infected with *Pb*-Luc in dynamic conditions at 2:1 and 1:1 cell/spz ratios. The infection rate is expressed as the percentage of bioluminescence normalized by micrograms of DNA relative to the infection in static conditions of 2.5×10^4 cell/well in a 1:1 cell/spz ratio. Data represent the mean \pm SEM of at least two independent experiments. (C) *Pb*-Luc development in HepG2 spheroids infected by *Pb*-Luc in dynamic conditions at a 2:1 cell/spz ratio. Data shown are bioluminescence values measured at 24, 36, 48, 60, and 70 hpi. Results are presented as mean \pm SEM of four independent experiments.

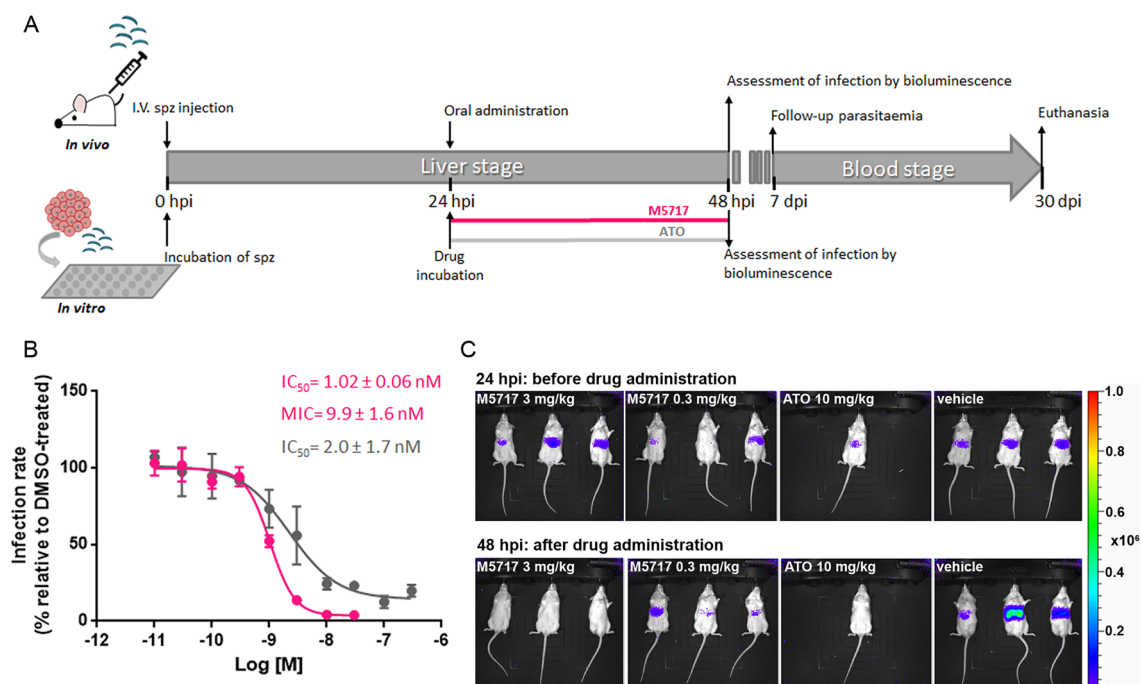


Figure 5. Preclinical assessment of M5717 dose–response (hpi, hours postinfection; dpi, days postinfection). (A) Schematic representation of drug administration *in vivo* and *in vitro* for IC₅₀ determination (not at scale). (B) Dose–response curves and IC₅₀ determinations of M5717 (pink) and atovaquone (ATO, gray) in HepG2 spheroids infected by *Pb*-Luc under static conditions at 2.5×10^4 cell/well in a 1:2 cell/spz ratio. Results are presented as the mean \pm SD of three independent experiments. (C) Ventral view images of NMRI mice infected with 100000 luciferase-expressing sporozoites before (24 h) and after (48 h) treatment with 3 mg/kg of M5717, 0.3 mg/kg of M5717, 10 mg/kg ATO, and vehicle. Heat maps of mice represent the intensities of bioluminescence (radiance, p/s/cm²/sr) as indicated by the pseudocolor scale.

1.1 \pm 0.2% infected cells, similar to the 0.9 \pm 0.3% infection rate observed for the higher 3D cell density employed (Figure 2B). No significant differences were observed among the different conditions employed for HC-04 cell infection, with

the percentage of infected cells ranging from 0.4 to 0.5% (Figure 2B). Parasite development, as estimated from the GFP geometric mean fluorescence intensity (MFI) at 48 hpi, was also not statistically different among all experimental

conditions (Figure 2C). At this time point, the presence of the protein up-regulated in infective sporozoites 4 (UIS4), a constituent of the parasitophorous vacuole membrane (PVM),³⁴ was detected inside HepG2 cells in the inner layers of the spheroids (Figure 2D). The parasite's hepatic development in HepG2 and HC-04 spheroids was further assessed throughout infection, at 24, 36, 48, and 60 hpi. *Pb* proliferated in the infected hepatocytes, as indicated by the increase in GFP MFI from 24 h onward (Figure 3A). These values peaked at 48 hpi in all cultures, only further increasing up to 60 hpi in adherent HepG2 cells (Figure 3A). These results were corroborated by immunofluorescence microscopy analyses, which showed an increase in hepatic parasite size up to 60 hpi (Figure 3B).

To evaluate the maturation of *Pb* parasites in HepG2 and HC-04 spheroids, merozoite release was assessed at 70 hpi in supernatants of 3D cultures. In all conditions, luciferase activity was detected on culture supernatants (Figure 3C), suggesting that parasites are able to mature into merozoites and be released from hepatic spheroids of both cell lines. To fully ascertain merozoite release and infectivity, HC-04 spheroid culture supernatants were then injected into BALB/c mice, and the ensuing appearance of blood parasitemia was monitored. The results showed that mice developed parasitemia from day 6 after supernatant injection onward, with all mice becoming blood stage positive at day 8 after injection (Table S2). Altogether, these results show that the 3D cultures of HepG2 and HC-04 cells are able to sustain invasion by *Pb* sporozoites, as well as parasite replication and differentiation. Furthermore, merozoites derived from HC-04 spheroids fully matured into blood-infective merozoites, leading to the onset of blood parasitemia following injection into mice.

Next, an alternative approach to static *Pb* infection, dynamic 3D infection, was established using HepG2 spheroids and *Pb*-Luc in stirred-tank vessels (Figure 4A). To promote the contact between spheroids and sporozoites, the former were cultured in suspension at high densities in a low culture volume during the 2 h required for *Pb* invasion (cell/spz ratios of 2:1 and 1:1).³² The infection of HepG2 spheroids in static conditions was used as a control (2.5×10^4 cell/well with a 1:1 cell/spz ratio). Under stirring conditions, the infection rate observed at 48 hpi with a 1:1 cell/spz ratio was $82 \pm 16\%$ of that of the control (Figure 4B). At 2:1 cell/spz, the infection rate was $60 \pm 19\%$ of that of the control. Bioluminescence values increased from 12 to 60 hpi, with a slight decrease at 70 hpi (Figure 4C), suggesting that the parasites could develop in dynamic culture. Collectively, these results demonstrate that *Plasmodium* invasion and development in HepG2 spheroids occurs in both static and dynamic conditions.

Suitability of 3D Infection Platforms for Evaluation of Dose- and Time-Dependent Responses to Antiplasmodial Drugs. To correlate the *in vitro* hepatic spheroid infection platforms with the *in vivo* rodent *Pb* model, the activity and concentrations of M5717 were assessed and compared in a similar protocol. Addition of compounds occurred 24 h after *Pb* infection of 3D HepG2 spheroids, and oral dosing was performed 24 h post sporozoite injection into mice. ATO was used as a positive control in these experiments (Figure 5A).

In vitro, the half maximal inhibitory concentration (IC_{50}) was determined using the 3D static infection platform. The range of concentrations employed did not impact cell viability at 48 hpi (Figure S3A). IC_{50} values for M5717 and ATO in infected HepG2 spheroids analyzed at 48 hpi were 1.0 ± 0.1

and 2.0 ± 1.7 nM, respectively. Also, the minimum inhibitory concentration (MIC) for M5717 was 9.9 ± 0.1 nM, corresponding to approximately 10 times the drug's IC_{50} value (Figure 5B). These results are in agreement with the IC_{50} values determined in the control 2D HepG2 cultures for M5717 and ATO (0.4 ± 0.3 and 1.9 ± 0.6 nM, respectively; Figure S3B).

In vivo, a single oral dose of 0.3 mg/kg failed to clear all liver stage parasites, whereas at 3 mg/kg M5717 was able to completely clear the *Pb* liver stage infection only 24 h after drug administration, with no recrudescence of parasites (monitored in the blood until day 33 post-treatment). As previously reported by Baragana et al.,⁹ ATO was able to clear parasites at a single oral dose of 10 mg/kg (Figure 5C).

To correlate the *in vivo* exposure with the 3D *in vitro* effective concentrations, the average plasma concentration (C_{av}) over 24 h was compared to the *in vitro* MIC. At 3 mg/kg, the plasma C_{av24h} was 61 nM and corresponded to 6-fold of the *in vitro* MIC (9.9 nM), whereas the noncurative dose of 0.3 mg/kg reached a C_{av} of 5 nM, which corresponded to only half of the MIC required *in vitro*.

To ascertain the platforms' translational potential and take full advantage of the 3D dynamic infection platform, which allowed long-term follow-up of the infected culture, the time-response of M5717 was assessed. Parasite inhibition in the dynamic 3D platform was assessed from 24 hpi with concentrations of M5717 above the MIC (25 nM) and below the MIC (1 nM). Both concentrations of M5717 showed inhibitory effects immediately after drug exposure at 24 hpi (Figure 6). Although *Pb* development was completely

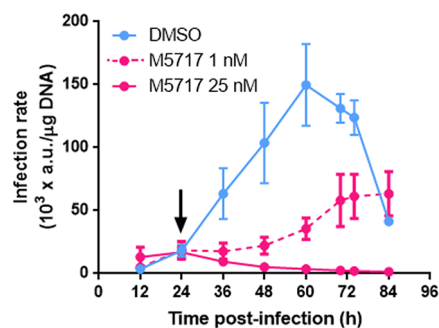


Figure 6. Time-response of M5717 in *Pb* infection. Time-response of M5717 was determined under stirred conditions in *Pb* infection of HepG2 spheroids. Results are expressed as arbitrary units of bioluminescence (a.u.) measured by luciferase activity per microgram of DNA and represent the mean \pm SEM of three independent experiments. The arrow indicates the time at which the drug was administered. M5717 was administered at 1 nM (pink dashed line) and 25 nM (pink line). The drug vehicle, DMSO, was administered as a control (blue line).

inhibited throughout the culture period at 25 nM M5717, a concentration of M5717 below the MIC (i.e., 1 nM) only partially inhibited *Pb* infection up to $79 \pm 2\%$ at 48 hpi.

DISCUSSION

The scarcity of accurate experimental models that adequately recapitulate the human hepatic phenotype, *Plasmodium* hepatic infection, and drug metabolism have hampered the development of drugs targeting the liver stages of the malaria parasite. We have previously shown that stirred-tank culture systems are suitable for generation of 3D hepatic cell models, which retain

a stable hepatic phenotype up to several weeks of culture.^{27,28} In the present work, spheroids of selected human hepatic cell lines were employed in the establishment of static and dynamic 3D infection platforms, which sustain infection by *Plasmodium* parasites and their complete development.

Two-dimensional cultures of hepatic cell lines have been extensively used as a model for the characterization of the liver stage of *Plasmodium* infection. More complex culture systems, relying on PHH cultured on natural matrixes (e.g., collagen I) or in coculture with murine fibroblasts to provide signaling cues and confer spatial restrictions to improve the hepatocyte phenotype, have also been employed for the assessment of *Plasmodium* infection and long-term parasite development.^{15,16} Resorting to the use of matrix components or microcarrier beads for 3D cultures of hepatic cells has been previously proposed for the study of another hepatotropic pathogen, the hepatitis C virus (HCV).^{35–37} Despite the advantages of these complex biological platforms over conventional 2D cultures, the presence of nonhuman and undefined components, the batch-to-batch variability of the materials, and the donor variability and high cost associated with PHH are disadvantages for their routine application. Conversely, cell-line-derived hepatic spheroids generated in stirred-tank vessels constitute a fully human cell model, that is robust and cost-effective for straightforward integration in screening platforms. In the present study, spheroids of three hepatic cell lines were generated in a stirred-tank culture system by tuning critical parameters, such as cell inoculum, agitation rate, and serum concentration.^{27,30} This process generated compact spheroids with an average diameter lower than 200 μm and did not generate necrotic centers in HepG2 spheroids.²² Furthermore, spheroids maintained cell viability for at least one month in culture. Moreover, we show that hepatic spheroids of HepG2 and HC-04 cell lines kept a stable hepatic phenotype, characterized by the expression of liver-specific proteins, albumin, and HNF4 α , and cell polarity, a crucial feature for liver function.¹⁸ Additionally, we have previously shown that hepatic spheroids secrete and accumulate extracellular matrix components that contribute to the long-term maintenance of hepatic phenotype.^{19,25} Therefore, hepatic spheroids recapitulate features of the liver architecture and metabolism.

Our results show that HepaRG cells could not be infected by *Pb*, similarly to what has been reported for the human-infective *Pf* and the monkey-infective *Plasmodium cynomolgi* parasite species, in which HepaRG cells were used as a negative control of infection¹⁴ or were not infected by *Pf* and *Pc* in coculture with PHH.¹¹ Conversely, HepG2 and HC-04 spheroids sustained *Pb* infection, in accordance with what is reported for 2D cultures.^{32,38} *Pb* was able to infect cells in both the outer and inner layers of the spheroids, suggesting that the 3D architecture does not compromise the cell traversal process and subsequent productive invasion. Parasite development inside the invaded hepatocytes was observed by the continuous increase in parasite size up to 48 hpi, at which time the presence of UIS4, an essential protein for parasite maturation throughout hepatic development,³⁴ showed full integrity of the PVM. The parasite maturation process, which *in vivo* culminates in the release of infectious merozoites to the bloodstream, was also replicated in the spheroid cultures, as shown by the detection of luminescence in the culture supernatant and the capability of the latter to initiate a blood stage infection in mice. Thus, besides displaying relevant hepatic architecture and polarization, hepatic spheroids sustain

complete *Plasmodium* hepatic infection. The 3D dynamic infection platform developed in this study took advantage of stirred-tank culture systems to maintain high cell densities for longer periods of time. In the dynamic conditions, the infection rates obtained were within the same range of the ones obtained in static conditions. Therefore, the developed 3D dynamic infection platform sustains efficient *Pb* infection of hepatic spheroids in a system that supports homogeneous distribution of all culture components, is scalable, and allows easy sampling and monitoring over time without compromising the continuity of the infected culture.

The newly generated static and dynamic platforms were further validated for drug testing. The determination of the IC₅₀ values of both M5717 and ATO showed that M5717 displays a higher inhibitory effect against *Plasmodium* hepatic infection than ATO, in agreement with a previous report by Baragana et al.⁹ Moreover, the translational potential of the 3D static platform was demonstrated by comparing effective concentrations of M5717 on *Pb* infection *in vitro* and *in vivo*. Using the *in vitro* 3D hepatic platform, we could show that concentrations as low as 10 nM, corresponding to the MIC, were efficient in clearing a patent liver infection. Furthermore, *in vivo* data demonstrated that average plasma concentrations over 24 h (C_{av}) greater than the MIC (i.e., 61 nM) were able to clear the liver infection, whereas doses of M5717 yielding C_{av} values lower than the MIC (i.e., 0.5 nM) failed to clear all parasites 48 hpi, resulting in detection of parasites in circulating blood. Because of the long-term maintenance and nondestructive, continuous sampling of the dynamic infection platform, we could follow up infected cultures after drug addition to ascertain the complete efficacy and exclude the possibility of remission. This was exemplified with M5717, which completely inhibited the progression of infection at a concentration greater than the MIC (i.e., 25 nM), whereas a concentration below the MIC (i.e., 1 nM) only partially inhibited *Pb* infection.

Beyond the translational potential from *in vitro* to *in vivo* and the drug screening uses, these platforms may also constitute an invaluable tool for studying the basic biology of *Plasmodium* hepatic infection in a physiologically relevant context, for instance, in understanding the mechanisms of cell traversal by *Plasmodium* sporozoites, a process whose role in infection remains unclear.^{2,39} Moreover, the platforms described in this work can potentially be translated to human *Plasmodium* parasites, as stirred-tank culture systems are suitable for spheroid culture of HC-04 cells and PHH, which sustain infection by *Pv* and *Pf*.^{14,27,40} Moreover, the long-term maintenance of stable hepatic phenotypes can be especially useful when investigating hypnozoites, dormant forms generated by *Pv* and *Po* parasites that persist in hepatocytes.^{11,12}

CONCLUSION

To the extent of our knowledge, we hereby report for the first time that *P. berghei* can infect and develop inside hepatic spheroids, completely maturing into blood-infective parasites. This 3D culture platform constitutes a promising tool for drug discovery targeting liver stages of *Plasmodium* infection. Besides recapitulating key features of liver cell function, the system can be scaled up to feed medium to high throughput platforms for drug screening purposes or to sustain *Plasmodium* infections in dynamic systems. With the possibility of long-term maintenance, medium culture exchange, and non-

destructive and continuous sampling, this technology allows the monitoring of infected cultures subjected to various culture conditions (e.g., hypoxia) or drug treatments, which is useful for translational medicine purposes (e.g., pharmacokinetic/pharmacodynamic modeling). The feasibility of using cell sources that support infection by a range of rodent- and human-infective parasites, combined with the possibility of performing dose–response and time–response studies, emphasizes the flexibility of these platforms. Collectively, these features highlight the potential of hepatic spheroids for addressing particular issues of host–parasite interaction, with the ultimate goal of identifying novel compounds that can be used for prophylactic or therapeutic interventions.

MATERIALS AND METHODS

Animal and Cell Sources. All animal experiments were performed in strict compliance with the guidelines of the animal ethics committee of Instituto de Medicina Molecular João Lobo Antunes (iMM, Lisboa, Portugal), which also approved the study, and the Federation of European Laboratory Animal Science Associations (FELASA). Male BALB/c mice (Charles River Laboratories), 6–8 weeks of age, were kept and manipulated in iMM's animal facility. The animal experiments carried out at the Swiss Tropical and Public Health Institute (SwissTPH, Basel, Switzerland) adhered to local and national regulations of laboratory animal welfare in Switzerland (awarded permission no. 2693). Protocols were regularly reviewed and revised following approval by the local authority (Veterinäramt Basel Stadt). Female NMRI mice (Charles River Laboratories), 20–22 g of body weight, were housed and manipulated in SwissTPH's animal facility. The hepatic cell lines used in this study were HC-04, HepG2, and HepaRG. The HC-04 cell line was obtained from Sanaria Inc., whereas the HepG2 and HepaRG cell lines were purchased from ATCC and Thermo Fisher Scientific, respectively.

2D Cell Culture. 2D cell cultures were maintained in static conditions. HepaRG cells were cultured as previously described.^{19,41} HepG2 and HC-04 cells were cultured in low glucose DMEM and DMEM/F12 supplemented with HEPES, respectively (both from Thermo Fisher Scientific). The culture medium of both cell lines was supplemented with 1% (v/v) penicillin/streptomycin and 10% (v/v) FBS. These cell lines were passaged twice every week at a cell inoculum of 5×10^4 and 4×10^4 cell/cm², respectively. All cell lines were routinely propagated in T-flasks under static conditions and maintained in an incubator with humidified environment at 37 °C with 5% CO₂.

3D Cell Culture (Spheroids). Hepatic cell spheroids were generated and maintained up to 30 days in dynamic suspension, with stirred vessels (125 or 30 mL spinner vessels from Corning, Merck KGaA, and ABLE Biott Corporation, respectively) placed on magnetic stirrers (2mag AG), and kept in an incubator with humidified environment at 37 °C with 5% CO₂. Single cell suspensions of 3×10^5 cell/mL were inoculated into the spinners in the culture medium employed for 2D cell culture supplemented with 10–20% (v/v) FBS. The agitation rates and the medium exchange regimens tailored for each cell line are described in the Supporting Information (Table S1). Medium replacement was performed by centrifugation, followed by cell pellet resuspension in fresh culture medium supplemented with 5–10% (v/v) FBS.

Production of *P. berghei* Sporozoites. Green fluorescent protein (GFP)- or luciferase (Luc)-expressing *P. berghei* (Pb) ANKA sporozoites reared in iMM's insectary and *P. berghei* mCherry ANKA-Luci-GFP reared at Swiss TPH's insectarium were employed. *Anopheles stephensi* mosquitoes employed at iMM were infected by feeding on infected mice as previously described.³⁸ At Swiss TPH's insectarium, the mosquitoes were obtained by feeding on infected female NMRI mice after 12–24 h of starvation (without glucose solution). Female *Anopheles stephensi* mosquitoes were allowed to feed on anaesthetized mice (Escornakon, pentobarbital in 15% ethanol, 70 mg/kg, injected intraperitoneally, ip) for 30 min, and blood-fed mosquitoes were reared with 8% fructose with 0.5% PABA and H₂O solution.

Salivary glands of infected *Anopheles stephensi* mosquitoes were freshly isolated into RPMI 1640 medium (Thermo Fisher Scientific) or phosphate-buffered saline (PBS), macerated with a micropistil and filtered through a 40 μm cell strainer to remove mosquito debris. The free sporozoites were then counted in a Bürker-Türk or Neubauer chamber using phase-contrast microscopy.

Plasmodium Infection of 2D Cultures. 2D cultures of HepG2, HC-04, and HepaRG cells were infected as previously described.^{38,42} Briefly, cells were plated at a density of 3.1×10^4 cell/cm² in 96-well plates the day before infection. The following day, the culture medium was replaced by infection medium (low glucose DMEM supplemented with 5% (v/v) FBS, 1:300 amphotericin B (250 μg/mL), and 1:1000 gentamycin (50 mg/mL), all from Thermo Fisher Scientific) and 1×10^4 sporozoites were added to each well, to achieve a cell/spz ratio of 1:1. In noninfected controls, medium was added in place of sporozoites. Sporozoite addition was followed by a centrifugation step at 1800g for 5 min, and plates were maintained in static conditions at 37 °C and 5% CO₂ for 2 h. After this period, an equal volume of fresh infection medium was added to the wells. The cultures were maintained in static conditions up to 48 h postinfection (hpi), at which time the infection rates were assessed either by detection of GFP by flow cytometry or by measurement of luciferase activity, as described below. For the assessment of parasite development throughout infection, 2D cultures were processed for flow cytometry, analyzed at 24, 36, 48, and 60 hpi. HepaRG and HC-04 infection values were normalized to those obtained with HepG2.

Plasmodium Infection of 3D Cultures. Prior to infection, the cell density of each dynamic spheroid culture was determined, as described below.

For static infections, spheroids from day 9 of culture were plated in ultralow attachment flat bottom 96-well plates (Corning, Merck KGaA) at 1×10^4 , 2.5×10^4 , and 5×10^4 cell/well densities, in a total volume of 100 μL. The infection procedure was performed as described for 2D cultures. The number of sporozoites was adjusted depending on the cell/spz ratio intended. For dynamic infection, a suspension spheroid culture was established at 5×10^5 or 1×10^6 cell/mL in 30 mL spinners from ABLE Biott Corporation. Sporozoite suspensions were added to attain cell/spz ratios of 1:1 and 2:1. The culture was maintained under constant stirring for 2 h, after which a 1:4 to 1:8 dilution was performed, and the culture was maintained up to 84 hpi. The infection medium for the static and dynamic infections was the same as that employed for 2D infection. A control condition of infection in 2D HepG2 cells was included in all experiments. For the assessment of parasite

infection rate and development throughout infection, spheroids were collected at 24, 36, 48, 60, and 70 hpi for flow cytometry and bioluminescence or immunofluorescence microscopy analysis, as described below.

Merozoite Infectivity Assessment *in Vivo*. BALB/c mice were infected by intravenous (iv) injection of 200 μL of supernatants collected from *Pb*-Luc-infected cells cultured in 2D and 3D static infection conditions. The supernatants from each condition were injected into five and four mice, respectively. A noninfected mouse was used as a negative control. Blood stage infections were monitored by analysis of Giemsa-stained blood smears and detection of GFP by flow cytometry in tail blood, collected between days 4 and 11 postinjection.

Characterization of Spheroid Cultures: Cell Viability, Concentration, and Spheroid Diameter. Cell viability was determined by a fluorescence live–dead assay, as previously described.⁴³ Briefly, spheroids were incubated with fluorescein diacetate (Sigma-Aldrich, Merck) at 10 $\mu\text{g}/\text{mL}$ for detection of viable cells and the DNA dye TO-PRO-3 iodide (Thermo Fisher Scientific) at 1 μM for detection of dead cells. FDA is a cell-permeant esterase substrate that measures both enzymatic activity, which is required to activate its fluorescence, and cell-membrane integrity, which is required for intracellular retention of the fluorescent product. TO-PRO-3 is a DNA dye that stains cells with compromised membranes. Spheroids were visualized in an inverted fluorescence microscope (Leica DMI6000). Cell concentrations were determined by the Trypan blue exclusion method, as described previously.¹⁹ Spheroid size was determined by measuring Feret's diameter⁴³ using the open source ImageJ software (version 1.52b).⁴⁴

Fluorescence Microscopy. Fluorescence microscopy of spheroids and adherent cells was performed as previously reported.²⁸ Briefly, cells were fixed in 4% (w/v) paraformaldehyde with 4% (w/v) sucrose in PBS for 20 min. For the generation of cryosections, spheroids were incubated in a solution of 30% (w/v) sucrose overnight and frozen in optimum cutting temperature (OCT) compound Tissue-Tek (Sakura) at $-80\text{ }^{\circ}\text{C}$. The frozen samples were sectioned in 10–40 μm slices using a Cryostat (Leica). For detection of intracellular epitopes, cryosections and adherent cells were processed for immunofluorescence with the following procedure: permeabilization with 0.1% (v/v) Triton X-100 (TX-100) and blocking with 0.2% (w/v) fish-skin gelatin (FSG) solution in PBS for 30 min. The incubation of primary antibodies (Abs) was performed for 2 h in a solution containing 0.125% (w/v) FSG and was followed by the incubation of secondary Abs for 1 h in the same solution. For F-actin detection, following permeabilization, a single incubation step of 20 min with A488- or TRITC-conjugated Phalloidin (A12379, Thermo Fisher Scientific, and P1951, Sigma-Aldrich, respectively) in PBS was performed. Finally, cryosections and adherent cells were mounted in DAPI-containing Prolong (P36935, Thermo Fisher Scientific). The primary antibodies used for immunodetection of hepatic phenotype included human serum albumin (Alb; Ab8940-1, Abcam) and hepatocyte nuclear factor 4 α (HNF4 α ; Ab41898, Abcam). For the characterization of infection, antibodies against *P. berghei* UIS4 protein (AB0042, SICGEN) and GFP (G6539, Merck) and mouse monoclonal antibody 2E6 against *Pb* heat shock protein 70 (*Pb*HSP70) were used. The samples were visualized using point scanning (SP5, Leica), spinning disk microscopy (Andor revolution $\times\text{D}$, Andor Technology

PLC) and LSM 710 confocal laser point scanning (Zeiss) microscopes.

Assessment of *Plasmodium* Infection by Flow Cytometry. *Pb*-GFP-infected samples were washed with PBS, trypsinized for determination of cell density, and resuspended in 70–150 μL of 2% (v/v) FBS in PBS. Blood from the tails of mice injected with the supernatants of infected cultures was collected to 2% (v/v) FBS in PBS. Cells were analyzed on a BD Accuri C6 or LSRFortessa (BD Biosciences) with the appropriate settings for the fluorophores used. Data acquisition and analysis were carried out using the Accuri C6 (version 1.0.264.21, BD), FACSDiva (version 6.2, BD), and FlowJo (version 10.0.8, FlowJo) software packages.

Assessment of *Plasmodium* Infection by Measurement of Luciferase Activity. *Pb*-Luc-infected cells were processed at time points ranging from 12 to 84 hpi, depending on the intended readout, for measurement of luciferase activity using the Firefly Luciferase Assay Kit (Biotium), following the manufacturer's instructions. Briefly, cells were washed twice with PBS, after which lysis buffer, diluted 1:4, was added. Cells were alternately frozen and thawed with agitation at 500 rpm until complete cell lysis. Bioluminescence was measured using a microplate reader (Infinite 200 PRO, Tecan Trading AG), and the light reaction of each well was measured for 100 ms.

Drug Assays. M5717 was synthesized as described in Baragaña et al.⁹ and supplied by Merck KGaA. Atovaquone (ATO) was bought from Merck (Sigma-Aldrich, A7986). Stock solutions of 10 mM were prepared in DMSO.

***In Vitro* Drug Assays.** Working solutions of compounds employed in drug assays were prepared fresh at concentrations ranging from 0.01 to 300 nM prior to incubation with cells. Infection of 2D HepG2 cell cultures with *Pb*-Luc was performed at 1×10^4 cell/well with a cell/spz ratio of 1:1. Infection of HepG2 spheroids in static conditions was performed at 2.5×10^4 cell/well at cell/spz ratios of 1:1 and 1:2, respectively, and infection in dynamic conditions was performed at 5×10^6 and 1×10^6 cell/mL at cell/spz ratios of 1:1 and 2:1, respectively. At 24 hpi, cells were exposed to the selected drug dilutions and cultured for an additional 24 h. For the construction of dose-dependency curves, infection rate and metabolic activity were assessed at 48 hpi, whereas for the time-dependent response studies, infection rate and dsDNA concentration were assessed up to 84 hpi. Cell metabolic activity was determined by PrestoBlue (Thermo Fisher Scientific) following the manufacturer's instructions. Briefly, cells were incubated with Presto Blue 1 \times for 50 min at $37\text{ }^{\circ}\text{C}$, and the fluorescence of the culture supernatant was measured by employing 560 and 590 nm excitation and emission wavelengths, respectively, using a microplate reader (Infinite 200 PRO, Tecan Trading AG). dsDNA quantification was performed following the manufacturer instruction's for the Quant-iT PicoGreen dsDNA Assay Kit (P7589, Thermo Fisher Scientific). Cell metabolic activity, which correlates to cell viability, was used as a normalization method for the infection rate in the IC_{50} determination assay, whereas DNA content was used to normalize infection rate in the time–response assessment *in vitro*. Cells were then analyzed for bioluminescence as previously described.

Nonlinear regression analysis was employed to fit the normalized results of the dose–response curves, and IC_{50} values were determined using GraphPad Prism version 6 for Windows (GraphPad Software). The lowest concentration of antiparasitic drug that inhibited infection by 99% relative to

DMSO-treated controls was considered the minimal inhibitory concentration.⁴⁵

In Vivo Drug Assays (Established Liver Infection). Naïve mice were infected with 1×10^5 sporozoites of *P. berghei* mCherry ANKA-Luci-GFP by iv injection in the tail vein. At -2 h or $+24$ hpi, single oral dose drug treatments with M5717 (0.3, 3, and 30 mg/kg, as indicated in Figure 5C) were given to groups of three mice. One mouse received 10 mg/kg ATO as a positive control, and three mice served as untreated controls (compounds were dissolved in a vehicle of 7% Tween 80 and 3% ethanol). At 23 and 48 hpi, liver-stage *Plasmodium* infection was assessed *in vivo* in all mice. To this end, mice were anesthetized with isoflurane after an iv injection of D-luciferin (30 mg/mL) in a volume of 5 mL/kg. To measure bioluminescence, which correlates with the degree of liver infection, anesthetized mice were placed in an IVIS Lumina II system, and images were acquired with a highly sensitive charge-coupled device (CCD) camera using LivingImage 4.3 Software. The generated heat maps of mice represent intensities of bioluminescence, with radiance ($\text{p/s/cm}^2/\text{sr}$) indicated by a pseudocolor scale ($\text{min} = 1.20 \times 10^4$ and $\text{max} = 1.00 \times 10^6$). At 7, 14, 17, 21, 24, 28, 31, and 35 days postinfection, blood-stage parasitemia was measured by light microscopy on Giemsa-stained blood smears, and positive mice were euthanized. Mice without detectable parasitemia until day 35 postinfection (33 days post-treatment) were considered as cured and were euthanized.

Blood-to-Plasma Ratio. M5717 was incubated at $1 \mu\text{M}$ for 30 min at 37°C in mouse whole blood as well as in control plasma (i.e., surrogate for whole blood). Whole blood samples were centrifuged to obtain plasma. M5717 concentrations in plasma supernatant and control plasma were quantified by LC-MS/MS. The blood-to-plasma ratio ($K_{B/P} = C_B/C_P$) was calculated on the basis of M5717/internal standard peak area ratios (PAR) according to the equation $K_{B/P} = \text{PAR}_{\text{p(control)}}/\text{PAR}_{\text{p}}$. The mouse C_B/C_P ratio for M5717 was found to be 3.27.

Data Analysis and Statistics. Statistical analysis was performed using GraphPad Prism version 6 for Windows (GraphPad Software). A parametric *t* test was performed, considering paired conditions when subjected to the same batch of spz. For unpaired conditions, one-way ANOVA followed by Tukey's multicomparisons test was performed. For statistically significant results, *p* values are presented ($*p < 0.05$, $**p < 0.01$, $***p < 0.001$, $****p < 0.0001$).

■ ASSOCIATED CONTENT

● Supporting Information

The Supporting Information is available free of charge on the ACS Publications website at DOI: 10.1021/acsinfecdis.9b00144.

Conditions for 3D culture of HepG2, HC-04, and HepaRG spheroids in stirred-tank systems; merozoite infectivity indicated by the number of blood stage positive mice at different times after injection of culture supernatants from HC-04 spheroids infected by *Pb*-GFP at a 1:2 cell/spz ratio; characterization of cellular polarization of HepG2 and HC-04 spheroids by detection of membrane E-cadherin at day 9 of culture; optimization of 3D infection conditions; and preclinical assessment of M5717 and ATO dose—response *in vitro* (PDF)

■ AUTHOR INFORMATION

Corresponding Authors

*E-mail: marques@ibet.pt (P.M.A.).

*E-mail: beatrice.greco@merckgroup.com (B.G.).

*E-mail: mprudencio@medicina.ulisboa.pt (M.P.).

ORCID

Thomas Spangenberg: 0000-0002-5654-8919

Paula M. Alves: 0000-0003-1445-3556

Author Contributions

F.A., S.P.R., and D.F. contributed equally. S.P.R., M.J.T.C., T.S., C.B., B.G., M.P., and P.M.A. conceptualized the study. F.A., S.P.R., D.F., D.S., M.M., T.S., C.B., M.R., and M.P. developed the methodology. F.A., S.P.R., D.F., L.B., C.F., and M.R. performed the formal analysis. F.A., S.P.R., D.F., D.S., T.R.M., M.M., and C.F. performed the investigation. F.A., S.P.R., and D.F. wrote the original draft. T.S., C.B., M.P., and P.M.A. reviewed and edited the manuscript. C.O. provided resources. B.G., M.P., and P.M.A. acquired funding. M.J.T.C., T.S., C.B., B.G., M.P., and P.M.A. supervised the research.

Notes

The authors declare the following competing financial interest(s): F.A., S.P.R., D.F., D.S., M.M., M.J.T.C., T.S., C.B., B.G., M.P., and P.M.A. are inventors on patent WO 2018162623. L.B., C.O., T.S., and B.G. are employees of Merck, which funded the work and provided novel compounds to be tested in the platforms developed in this work.

■ ACKNOWLEDGMENTS

We gratefully acknowledge Dr. Ana Terraso for discussions on the *in vitro* drug assays performed in this work. We acknowledge Ana Filipa Teixeira and Ana Parreira for mosquito production and infection. We acknowledge Merck KGaA, Darmstadt, Germany, for funding the work. M.P. is a recipient of a “CEEC2017 FCT” award of Fundação para a Ciência e Tecnologia, Portugal (FCT) and was funded by FCT grant 02/SAICT/2017/29550. F.A. is the recipient of Ph.D. fellowship PD/BD/128371/2017, funded by FCT.

■ REFERENCES

- (1) (2018) *World malaria report 2018*, World Health Organization.
- (2) Mota, M. M., Hafalla, J. C. R., and Rodriguez, A. (2002) Migration through host cells activates Plasmodium sporozoites for infection. *Nat. Med.* 8 (11), 1318–1322.
- (3) Prudêncio, M., Rodriguez, A., and Mota, M. M. (2006) The silent path to thousands of merozoites: the Plasmodium liver stage. *Nat. Rev. Microbiol.* 4 (11), 849–856.
- (4) Wells, T. N. C., Burrows, J. N., and Baird, J. K. (2010) Targeting the hypnozoite reservoir of Plasmodium vivax: the hidden obstacle to malaria elimination. *Trends Parasitol.* 26 (3), 145–151.
- (5) Raphemot, R., Posfai, D., and Derbyshire, E. R. (2016) Current therapies and future possibilities for drug development against liver-stage malaria. *J. Clin. Invest.* 126 (6), 2013–2020.
- (6) Sridaran, S., McClintock, S. K., Syphard, L. M., Herman, K. M., Barnwell, J. W., and Udhayakumar, V. (2010) Anti-folate drug resistance in Africa: Meta-analysis of reported dihydrofolate reductase (dhfr) and dihydropteroate synthase (dhps) mutant genotype frequencies in African Plasmodium falciparum parasite populations. *Malar. J.* 9 (1), 247.
- (7) Burrows, J. N., Duparc, S., Gutteridge, W. E., Hooft van Huijsduijnen, R., Kaszubska, W., Macintyre, F., Mazzuri, S., Möhrle, J. J., and Wells, T. N. C. (2017) New developments in anti-malarial target candidate and product profiles. *Malar. J.* 16 (1), 26.
- (8) Palmer, M. J., and Wells, T., Eds. (2012) *Neglected Diseases and Drug Discovery*, Royal Society of Chemistry, Cambridge, U.K.

- (9) Baragana, B., Hallyburton, I., Lee, M. C. S., Norcross, N. R., Grimaldi, R., Otto, T. D., Proto, W. R., Blagborough, A. M., Meister, S., Wirjanata, G., Ruecker, A., Upton, L. M., Abraham, T. S., Almeida, M. J., Pradhan, A., Porzelle, A., Martinez, M. S., Bolscher, J. M., Woodland, A., Luksch, T., Norval, S., Zuccotto, F., Thomas, J., Simeons, F., Stojanovski, L., Osuna-Cabello, M., Brock, P. M., Churcher, T. S., Sala, K. A., Zakutansky, S. E., Jimenez-Diaz, M. B., Sanz, L. M., Riley, J., Basak, R., Campbell, M., Avery, V. M., Sauerwein, R. W., Dechering, K. J., Noviyanti, R., Campo, B., Frearson, J. A., Angulo-Barturen, I., Ferrer-Bazaga, S., Gamo, F. J., Wyatt, P. G., Leroy, D., Siegl, P., Delves, M. J., Kyle, D. E., Wittlin, S., Marfurt, J., Price, R. N., Sinden, R. E., Winzeler, E. A., Charman, S. A., Bebrevska, L., Gray, D. W., Campbell, S., Fairlamb, A. H., Willis, P. A., Rayner, J. C., Fidock, D. A., Read, K. D., and Gilbert, I. H. (2015) A novel multiple-stage antimalarial agent that inhibits protein synthesis. *Nature* 522 (7556), 315–320.
- (10) Okombo, J., and Chibale, K. (2017) Insights into Integrated Lead Generation and Target Identification in Malaria and Tuberculosis Drug Discovery. *Acc. Chem. Res.* 50 (7), 1606–1616.
- (11) Dembélé, L., Franetich, J., Lorthiois, A., Gego, A., Zeeman, A., Kocken, C. H. M., Le Grand, R., Dereuddre-Bosquet, N., van Gemert, G., Sauerwein, R., Vaillant, J., Hannoun, L., Fuchter, M. J., Diagona, T. T., Malmquist, N. A., Scherf, A., Snounou, G., and Mazier, D. (2014) Persistence and activation of malaria hypnozoites in long-term primary hepatocyte cultures. *Nat. Med.* 20 (3), 307–312.
- (12) March, S., Ng, S., Velmurugan, S., Galstian, A., Shan, J., Logan, D. J., Carpenter, A. E., Thomas, D., Sim, B. K. L., Mota, M. M., Hoffman, S. L., and Bhatia, S. N. (2013) A microscale human liver platform that supports the hepatic stages of plasmodium falciparum and vivax. *Cell Host Microbe* 14 (1), 104–115.
- (13) Gural, N., Mancio-Silva, L., Miller, A. B., Galstian, A., Butty, V. L., Levine, S. S., Patrapuvich, R., Desai, S. P., Mikolajczak, S. A., Kappe, S. H. I., Fleming, H. E., March, S., Sattabongkot, J., and Bhatia, S. N. (2018) In Vitro Culture, Drug Sensitivity, and Transcriptome of Plasmodium Vivax Hypnozoites. *Cell Host Microbe* 23 (3), 395–406.e4.
- (14) Roth, A., Maher, S. P., Conway, A. J., Ubalee, R., Chaumeau, V., Andolina, C., Kaba, S. A., Vantaux, A., Bakowski, M. A., Thomson-Louque, R., Adapa, R., Singh, N., Barnes, S. J., Cooper, C. A., Rouillier, M., McNamara, C. W., Mikolajczak, S. A., Sather, N., Witkowski, B., Campo, B., Kappe, S. H. I., Lanar, D. E., Nosten, F., Davidson, S., Jiang, R. H. Y., Kyle, D. E., and Adams, J. H. (2018) A comprehensive model for assessment of liver stage therapies targeting Plasmodium vivax and Plasmodium falciparum. *Nat. Commun.* 9 (1), 1837.
- (15) Hoffmaster, K. A., Turncliff, R. Z., LeCluyse, E. L., Kim, R. B., Meier, P. J., and Brouwer, K. L. R. (2004) P-glycoprotein expression, localization, and function in sandwich-cultured primary rat and human hepatocytes: relevance to the hepatobiliary disposition of a model opioid peptide. *Pharm. Res.* 21 (7), 1294–1302.
- (16) Khetani, S. R., and Bhatia, S. N. (2008) Microscale culture of human liver cells for drug development. *Nat. Biotechnol.* 26 (1), 120–126.
- (17) Dunn, J. C. Y., Tompkins, R. G., and Yarmush, M. L. (1992) Hepatocytes in collagen sandwich: Evidence for transcriptional and translational regulation. *J. Cell Biol.* 116 (4), 1043–1053.
- (18) Zeigerer, A., Wuttke, A., Marsico, G., Seifert, S., Kalaidzidis, Y., and Zerial, M. (2017) Functional properties of hepatocytes in vitro are correlated with cell polarity maintenance. *Exp. Cell Res.* 350 (1), 242–252.
- (19) Rebelo, S. P., Costa, R., Estrada, M., Shevchenko, V., Brito, C., and Alves, P. M. (2015) HepaRG microencapsulated spheroids in DMSO-free culture: novel culturing approaches for enhanced xenobiotic and biosynthetic metabolism. *Arch. Toxicol.* 89 (July), 1347–1358.
- (20) Gunness, P., Mueller, D., Shevchenko, V., Heinze, E., Ingelman-Sundberg, M., and Noor, F. (2013) 3D organotypic cultures of human heparg cells: A tool for in vitro toxicity studies. *Toxicol. Sci.* 133 (1), 67–78.
- (21) Chang, T. T., and Hughes-Fulford, M. (2009) Monolayer and Spheroid Culture of Human Liver Hepatocellular Carcinoma Cell Line Cells Demonstrate Distinct Global Gene Expression Patterns and Functional Phenotypes. *Tissue Eng., Part A* 15 (3), 559–567.
- (22) Gaskell, H., Sharma, P., Colley, H. E., Murdoch, C., Williams, D. P., and Webb, S. D. (2016) Characterization of a functional C3A liver spheroid model. *Toxicol. Res. (Cambridge, U. K.)* 5 (4), 1053–1065.
- (23) Gerets, H. H. J., Tilmant, K., Gerin, B., Chanteux, H., Depelchin, B. O., Dhalluin, S., and Atienzar, F. A. (2012) Characterization of primary human hepatocytes, HepG2 cells, and HepaRG cells at the mRNA level and CYP activity in response to inducers and their predictivity for the detection of human hepatotoxins. *Cell Biol. Toxicol.* 28 (2), 69–87.
- (24) Ramaiahgari, S. C., Den Braver, M. W., Herpers, B., Terpstra, V., Commandeur, J. N. M., Van De Water, B., and Price, L. S. (2014) A 3D in vitro model of differentiated HepG2 cell spheroids with improved liver-like properties for repeated dose high-throughput toxicity studies. *Arch. Toxicol.* 88 (5), 1083–1095.
- (25) Leite, S. B., Wilk-Zasadna, I., Zaldivar, J. M., Airola, E., Reis-Fernandes, M. A., Mennecozzi, M., Guguen-Guillouzo, C., Chesne, C., Guillou, C., Alves, P. M., and Coecke, S. (2012) Three-dimensional HepaRG model as an attractive tool for toxicity testing. *Toxicol. Sci.* 130 (1), 106–116.
- (26) Ramaiahgari, S. C., Waidyanatha, S., Dixon, D., DeVito, M. J., Paules, R. S., and Ferguson, S. S. (2017) Three-dimensional (3D) HepaRG spheroid model with physiologically relevant xenobiotic metabolism competence and hepatocyte functionality for liver toxicity screening. *Toxicol. Sci.* 159 (1), 124–136.
- (27) Tostões, R. M., Leite, S. B., Serra, M., Jensen, J., Björquist, P., Carrondo, M. J. T., Brito, C., and Alves, P. M. (2012) Human liver cell spheroids in extended perfusion bioreactor culture for repeated-dose drug testing. *Hepatology* 55, 1227–1236.
- (28) Rebelo, S. P., Costa, R., Silva, M. M., Marcelino, P., Brito, C., and Alves, P. M. (2017) Three-dimensional co-culture of human hepatocytes and mesenchymal stem cells: improved functionality in long-term bioreactor cultures. *J. Tissue Eng. Regen. Med.* 11 (7), 2034–2045.
- (29) Serra, M., Brito, C., Correia, C., and Alves, P. M. (2012) Process engineering of human pluripotent stem cells for clinical application. *Trends Biotechnol.* 30 (6), 350–359.
- (30) Santo, V. E., Estrada, M. F., Rebelo, S. P., Abreu, S., Silva, I., Pinto, C., Veloso, S. C., Serra, A. T., Boghaert, E., Alves, P. M., and Brito, C. (2016) Adaptable stirred-tank culture strategies for large scale production of multicellular spheroid-based tumor cell models. *J. Biotechnol.* 221, 118–129.
- (31) Sattabongkot, J., Yimamnuaychoke, N., Leelaudomlipi, S., Rasameesoraj, M., Jenwithisuk, R., Coleman, R. E., Udomsangpetch, R., Cui, L., and Brewer, T. G. (2006) Establishment of a human hepatocyte line that supports in vitro development of the exoerythrocytic stages of the malaria parasites Plasmodium falciparum and P. vivax. *Am. J. Trop. Med. Hyg.* 74 (5), 708–715.
- (32) Prudêncio, M., Mota, M. M., and Mendes, A. M. (2011) A toolbox to study liver stage malaria. *Trends Parasitol.* 27 (12), 565–574.
- (33) Prudêncio, M., Rodrigues, C. D., Ataíde, R., and Mota, M. M. (2007) Dissecting in vitro host cell infection by Plasmodium sporozoites using flow cytometry. *Cell Microbiol.* 10, 218–224.
- (34) Mueller, A.-K., Camargo, N., Kaiser, K., Andorfer, C., Frevert, U., Matuschewski, K., and Kappe, S. H. I. (2005) Plasmodium liver stage developmental arrest by depletion of a protein at the parasite-host interface. *Proc. Natl. Acad. Sci. U. S. A.* 102 (8), 3022–3027.
- (35) Aly, H. H., Shimotohno, K., and Hijikata, M. (2009) 3D cultured immortalized human hepatocytes useful to develop drugs for blood-borne HCV. *Biochem. Biophys. Res. Commun.* 379 (2), 330–334.
- (36) Molina-Jimenez, F., Benedicto, I., Dao Thi, V. L., Gondar, V., Lavillette, D., Marin, J. J., Briz, O., Moreno-Otero, R., Aldabe, R., Baumert, T. F., Cosset, F., Lopez-Cabrera, M., and Majano, P. (2012)

Matrigel-embedded 3D culture of Huh-7 cells as a hepatocyte-like polarized system to study hepatitis C virus cycle. *Virology* 425 (1), 31–39.

(37) Sainz, B., TenCate, V., and Uprichard, S. L. (2009) Three-dimensional Huh7 cell culture system for the study of Hepatitis C virus infection. *Virol. J.* 6 (1), 103.

(38) Ploemen, I. H. J., Prudencio, M., Douradinha, B. G., Ramesar, J., Fonager, J., van Gemert, G.-J., Luty, A. J. F., Hermsen, C. C., Sauerwein, R. W., Baptista, F. G., Mota, M. M., Waters, A. P., Que, I., Lowik, C. W. G. M., Khan, S. M., Janse, C. J., and Franke-Fayard, B. M. D. (2009) Visualisation and quantitative analysis of the rodent malaria liver stage by real time imaging. *PLoS One* 4 (11), e7881.

(39) Risco-Castillo, V., Topçu, S., Marinach, C., Manzoni, G., Bigorgne, A. E., Briquet, S., Baudin, X., Lebrun, M., Dubremetz, J., and Silvie, O. (2015) Malaria sporozoites traverse host cells within transient vacuoles. *Cell Host Microbe* 18, 593–603.

(40) Dumoulin, P. C., Trop, S a., Ma, J., Zhang, H., Sherman, M a., and Levitskaya, J. (2015) Flow cytometry based detection and isolation of Plasmodium falciparum liver stages in vitro. *PLoS One* 10, e0129623.

(41) Gripon, P., Rumin, S., Urban, S., Le Seyec, J., Glaise, D., Cannie, I., Guyomard, C., Lucas, J., Trepo, C., and Guguen-Guillouzo, C. (2002) Infection of a human hepatoma cell line by hepatitis B virus. *Proc. Natl. Acad. Sci. U. S. A.* 99 (24), 15655–15660.

(42) Machado, M., Sanches-Vaz, M., Cruz, J. P., Mendes, A. M., and Prudêncio, M. (2017) Inhibition of Plasmodium Hepatic Infection by Antiretroviral Compounds. *Front. Cell. Infect. Microbiol.* 7 (July), 1–9.

(43) Estrada, M. F., Rebelo, S. P., Davies, E. J., Pinto, M. T., Pereira, H., Santo, V. E., Smalley, M. J., Barry, S. T., Gualda, E. J., Alves, P. M., Anderson, E., and Brito, C. (2016) Modelling the tumour micro-environment in long-term microencapsulated 3D co-cultures recapitulates phenotypic features of disease progression. *Biomaterials* 78, 50–61.

(44) Rueden, C. T., Schindelin, J., Hiner, M. C., DeZonia, B. E., Walter, A. E., Arena, E. T., and Eliceiri, K. W. (2017) ImageJ2: ImageJ for the next generation of scientific image data. *BMC Bioinf.* 18 (1), 529.

(45) Russell, B. M., Udomsangpetch, R., Rieckmann, K. H., Kotecka, B. M., Coleman, R. E., and Sattabongkot, J. (2003) Simple In Vitro Assay for Determining the Sensitivity of. *Antimicrob. Agents Chemother.* 47 (1), 170–173.